

# Turbulence of generalised flows in two dimensions

Simon Thalabard <sup>1</sup>† and Jérémie Bec<sup>2,3</sup>

<sup>1</sup>Instituto Nacional de Matemática Pura e Aplicada, IMPA, 22460-320 Rio de Janeiro, Brazil

<sup>2</sup>Université Côte d’Azur, CNRS, OCA, Laboratoire J.-L. Lagrange, Nice, France

<sup>3</sup>MINES ParisTech, PSL Research University, CNRS, CEMEF, Sophia-Antipolis, France

(Received xx; revised xx; accepted xx)

This paper discusses the generalised least-action principle and the associated concept of generalised flow introduced by Brenier (*J. Am. Math. Soc.* 1989), from the perspective of turbulence modelling. In essence, Brenier’s generalised least-action principle extends to a probabilistic setting Arnold’s geometric interpretation of ideal fluid mechanics, whereby strong solutions to the Euler equations are deduced from minimising an action over Lagrangian maps. While Arnold’s framework relies on the deterministic concept of Lagrangian flow, Brenier’s least-action principle describes solutions to the Euler equations in terms of non-deterministic *generalised flows*, namely probability measures over sets of Lagrangian trajectories.

In concept, generalised flows seem naturally fit to describe turbulent Lagrangian trajectories in terms of stochastic processes, an approach that originates from Richardson’s seminal work on turbulent dispersion. This appears to be particularly suited to address cases when the concept of Lagrangian flows breaks down, due to Lagrangian trajectories being *spontaneously stochastic*. In practice though, Brenier’s generalised least-action principle has so far hardly found any practical application in the realm of fluid mechanics, let alone for turbulence modelling. The purpose of the present paper is therefore to give a *physical* perspective on Brenier’s principle, and provide a qualitative description of the hydrodynamical features of generalised flows. The exposition is guided by three questions: (i) Are generalised flows physically relevant? (ii) Do they exhibit turbulent properties? (iii) Can generalised least-action principles reproduce inertial-range dynamics? To address those points, a statistical-mechanics interpretation of Brenier’s principle is introduced, and Monte-Carlo techniques are employed to analyse the statistical features of three classes of two-dimensional generalised flows. The generalised least-action principle is then used to reconstruct some Eulerian and Lagrangian dynamics of increasing complexity, ranging from solid rotation, cellular (Beltrami) flows to freely decaying two-dimensional turbulence.

Our analysis highlights the fact that generalised flows are irrelevant when used over time lags that are larger than a prescribed threshold, which we interpret as a hydrodynamic turnover time. This “defect” is not specifically inherent to Brenier’s formulation, but rather to the variational framework being formulated as a two-end boundary-value problem. For small time lags, though, we argue that generalised flows are relevant and even capture turbulent features. Our results suggest that generalised variational formulations are of relevance for the purpose of turbulence modelling, and may even provide new tools to coarse-grain fully turbulent dynamics.

**Key words:** Variational methods, Turbulence modelling, Generalised flows

† Email address for correspondence: simon.thalabard@ens-lyon.org

## 1. Introduction

In the Lagrangian framework, incompressible ideal fluids can be pictured as freely evolving space-filling assemblies of infinitely-many classical “fluid particles”, whose internal energies are neglected, and whose collective dynamics is therefore conservative. It may hence come as no surprise that the Euler equations can be formally deduced from a Lagrangian least-action principle, whereby the action is the time integral of the total kinetic energy, while incompressibility appears as a non-holonomic constraint for the Lagrangian map  $(\mathbf{a}, t) \mapsto \mathbf{X}(\mathbf{a}, t)$ , which is assumed to be a smooth function of both time and the Lagrangian coordinates  $\mathbf{a}$ .

The deterministic Lagrangian least-action principle was made rigorous by Arnold (1966)—see also Khesin & Arnold (2005); Arnold (2013). It is at the root of the subsequent classical literature on Hamiltonian formulation of ideal fluid dynamics, which has found widespread ramifications in the context of geophysical and plasma modeling—we refer the reader to the pedagogical reviews by Shepherd (1990), Morrison (1998), Salmon (1988), and references therein. To briefly emphasise the power of least-action principles, let us here just point out that Hamiltonian methods not only provide a practical guideline that can be used to control approximations in asymptotic models (Holm & Kupershmidt 1983; Salmon 1983, 1985; Morrison 2005) and develop faithful numerical methods (Marsden & West 2001; Zeitlin 2004; Kraus *et al.* 2016), but also lay the basis for systematic stability analysis (Holm *et al.* 1985; Abarbanel *et al.* 1986) and formal statistical mechanics computations (Robert & Sommeria 1991; Miller *et al.* 1992; Bouchet & Corvellec 2010; Bouchet & Venaille 2012). In spite of its relevance when formally putting viscosity to zero, Arnold’s Lagrangian formulation is not necessarily appropriate in the context of turbulence, that is to describe solutions to the Navier–Stokes equations in the limit of vanishing viscosity.

From a mathematical viewpoint, Arnold’s least-action principle yields spatially smooth solutions to the Euler equations. Yet, it is well known that the notion of solution to the Euler equations needs to be carefully weakened in order to craft velocity fields that reproduce hallmark turbulent features while remaining physical (see, e.g., Duchon & Robert 2000; Eyink 2002). To that end, the notion of distributional solution with prescribed Hölder spatial regularity has been particularly scrutinised in relation to a conjecture made by Onsager (1949)—see also Eyink & Sreenivasan (2006). It has been recently established (Buckmaster 2015; Buckmaster *et al.* 2016; Isett 2018) that dissipative distributional solutions to the Euler equations do exist with a spatial Hölder exponent slightly below  $1/3$ . This indicates that an inviscid dynamics could indeed be relevant to reproduce experimental measurements, including the persistence of a finite dissipation in the limit of infinite Reynolds number (the so-called “dissipative anomaly”, see Sreenivasan 1984), the  $4/5$  law (see, e.g., Antonia & Burattini 2006), and possibly deviations to Kolmogorov 1941 scaling (see, e.g., Saw *et al.* 2018). It cannot be ruled out that constructing physical solutions to the Euler equation requires considering even weaker notions of solutions, examples of which include measure-valued solutions of DiPerna & Majda (1987)—see also Brenier *et al.* (2011)—where the local velocity is not uniquely defined but rather prescribed by a local probability distribution, namely a Young measure.

At a physical level, a crucial consequence of the velocity being probabilistic is that

fluid-element trajectories become themselves probabilistic: The concept of Lagrangian flow breaks down. A similar consequence is conjectured to also hold true for the rough velocity fields imagined by Onsager: This relates to the phenomenon of Lagrangian “spontaneous stochasticity” that was first formalized in the context of Kraichnan’s model for turbulent advection by Gawędzki (2001) — see also Falkovich *et al.* (2001). Clearly, a Lagrangian least-action principle built from the deterministic notion of Lagrangian map cannot reproduce such an expected intrinsic stochasticity of fluid trajectories. To that end, the generalised Lagrangian least-action principle formulated by Brenier (1989) could however be of particular relevance. Brenier’s formulation is essentially a probabilistic generalisation of Arnold’s principle. Roughly said, it consists in minimising a suitably-defined average kinetic energy among a very wide class of stochastic processes — the so-called “generalised Lagrangian flows” — rather than among the sole deterministic class of smooth diffeomorphisms. This generalisation guarantees the existence of minimisers under rather weak assumptions. Specifically, the minimising *generalised flow* is defined as a probability distribution on the space of Lagrangian paths. The solution is obtained by prescribing boundary conditions in time, which amounts to specifying the Lagrangian transition probabilities from the initial to the final time. This formulation of the problem is rooted in optimal transport and control theories (see for instance Villani 2009): Brenier’s formulation resembles a Kantorovich optimisation while Arnold’s formulation is essentially “Monge-like”.

Brenier’s least-action principle hence retains the desirable power of variational formulations, while embedding Arnold’s principle into a Lagrangian probabilistic framework, hereby making it compatible with the conjectured turbulent breakdown of Lagrangian flows. However, Brenier’s generalised flows were, to our knowledge, essentially discussed so far from a mathematical perspective (Brenier 1989, 1999, 2008): in connection to classical solutions and Arnold’s principle on the one hand, and in connection with weak dissipative Euler solutions on the other hand (Shnirelman 2000). More recently, explicit constructions of generalised flows were also used as test-bed setups for advanced numerical methods in multi-marginal optimal transport (Benamou *et al.* 2017; Mériçot & Mirebeau 2016; Gallouët & Mériçot 2018).

The purpose of the present paper is to give a *physical* perspective on Brenier’s least action principle, and provide a qualitative description of the hydrodynamical features of generalised flows, in relation to turbulence modelling. More specifically, our exposition is guided by the three following questions: *(i)* Are generalised flows physically relevant? *(ii)* Do they exhibit turbulent properties? *(iii)* Can generalised least-action principles reproduce inertial-range dynamics? To address those, we use a statistical mechanics interpretation of Brenier’s principle, to construct numerically specific instances of two-dimensional generalised flows, and analyse their Eulerian and Lagrangian statistical features. The answers to the first two questions turn out to depend on the specific time lag over which the variational principle is solved. We give evidence that generalised flows are irrelevant when the time lag is larger than a prescribed threshold, which we interpret as a hydrodynamic turnover time. This “defect” is not specifically inherent to Brenier’s formulation, but rather to the boundary-value variational framework itself: When solved over large time lags, Arnold’s least action principle also breaks down and produces incorrect Euler solutions. For small time lags, though, we argue that generalised flows are relevant and may even capture turbulent features. We illustrate this by reconstructing coarse-grained data from a decaying two-dimensional simulation. Our results suggest that generalised variational formulations are of relevance for the

purpose of turbulence modelling, and may even provide new practical ideas to reconstruct intermediate dynamics from turbulent datasets.

The paper is organised as follows. In §2 we formulate Arnold’s and Brenier’s least-action principles in a fluid-mechanical language. In §3 we provide a discrete version of generalised flows that allows for numerical constructions based on Monte-Carlo techniques. In §4 we use this method with, as input data, a coarse-grained Lagrangian map associated to Beltrami (cellular) flows. By investigating the time variations of kinetic energy, the scaling properties of the velocity field and Lagrangian trajectories, we argue that generalised flows display non-physical features when the time lag between the initial and final times is too large. We then use such considerations to investigate the case of two-dimensional decaying turbulence in §5. We observe that the generalised least-action principle allows to reconstruct the coarse-grained velocity when the time lag is chosen of the order or smaller than the large-eddy turnover time. Finally, we draw concluding remarks in §6.

## 2. Lagrangian variational formulations of inviscid fluid dynamics

### 2.1. Arnold’s least-action principle

In order to set the framework for Brenier’s formulation, let us first formally restate Arnold’s variational formulation of ideal fluid dynamics. Beyond the virtue of setting up some notations, we will then already be in a position to comment on the existence of a critical time-lag  $t_*$ , over which Arnold’s *least-action* principle becomes a weaker principle of *stationary action*: This unwanted feature will have a counterpart in Brenier’s formulation. To focus on general physical ideas, our exposition is intentionally phenomenological, and we refer the mathematically inclined reader to the book of Khesin & Arnold (2005) and the review of Ebin & Marsden (1970).

Arnold’s formulation is rooted on the deterministic Lagrangian viewpoint. The fluid is then nothing but the collection of individual fluid particles, which are labelled by some Lagrangian set of coordinates  $\mathbf{a}$ , and whose trajectories determine its dynamics. The formalisation uses the concept of Lagrangian flow map  $(\mathbf{a}, t) \mapsto \mathbf{X}(\mathbf{a}, t)$ , which associates to each fluid particle its position at time  $t$  within the physical domain  $\mathcal{D}$ . The projections  $\mathbf{a} \mapsto \mathbf{X}(\mathbf{a}, t)$  define the Lagrangian maps at time  $t$ , and the projections  $t \mapsto \mathbf{X}(\mathbf{a}, t)$  define the trajectories of particles with Lagrangian label  $\mathbf{a}$ . The Lagrangian flows are assumed to be smooth functions of both time and the Lagrangian coordinates. It is convenient to identify Lagrangian labels with the initial positions of fluid elements, so that  $\mathbf{X}(\mathbf{a}, 0) = \mathbf{a}$ . Hence, in the sequel, the initial map will always be taken as identity.

Lagrangian flows describe incompressible fluids when they preserve volumes, that is when the Jacobian determinant of the Lagrangian map satisfies  $|\partial\mathbf{X}/\partial\mathbf{a}| \equiv 1$ . The Eulerian velocity field is then obtained from the particle velocities through  $\mathbf{v}(\mathbf{X}(\mathbf{a}, t), t) = \partial_t\mathbf{X}(\mathbf{a}, t)$ . The total fluid kinetic energy therefore reads

$$\mathcal{E}(t) := \int_{\mathcal{D}} d\mathbf{a} \frac{1}{2} \|\partial_t\mathbf{X}(\mathbf{a}, t)\|^2. \quad (2.1)$$

Arnold’s Variational Principle can now be stated as

$$\begin{aligned} \mathcal{A}_{0, t_f}[\mathbf{X}(\cdot)] &:= \int_0^{t_f} dt \mathcal{E}(t) \longrightarrow \inf && \text{subject to} \\ \mathbf{X}(\cdot, 0) &= \mathbf{I}, \quad \mathbf{X}(\cdot, t_f) = \mathbf{X}_f(\cdot), \text{ and } \left| \frac{\partial\mathbf{X}}{\partial\mathbf{a}} \right| \equiv 1. && \text{(AVP)} \end{aligned}$$

The action functional  $\mathcal{A}_{0,t_f}$  appears as a natural counterpart to the actions used in textbooks for the formulation of classical finite-dimensional mechanics (see, e.g., José & Saletan 2000). It is obvious but worth emphasising, that the formulation (AVP) defines a *boundary-value* optimisation problem, as both “end-point” maps  $\mathbf{X}(\cdot, 0) = \mathbf{I}$  and  $\mathbf{X}_f(\cdot)$  at final time  $t_f$  are prescribed. A formal way of solving (AVP) is to use a Lagrange multiplier  $P(\mathbf{a}, t)$  to enforce the incompressibility constraint, and compute the functional derivatives with respect to the flow  $\mathbf{X}$  of the augmented action  $\mathcal{A}_{0,t_f} + \int_0^{t_f} dt \int_{\mathcal{D}} d\mathbf{a} P(\mathbf{a}, t) (|\partial\mathbf{X}/\partial\mathbf{a}| - 1)$ . The optimal solutions necessarily solve the Euler-Lagrange equations. Requiring the action to be stationary ( $\delta\mathcal{A}_{0,t_f} = 0$ ), a string of formal calculations leads to

$$\partial_{tt}\mathbf{X}(\mathbf{a}, t) = -[\partial\mathbf{X}/\partial\mathbf{a}]^{-1} \nabla_{\mathbf{a}} P, \quad \text{with } |\partial\mathbf{X}/\partial\mathbf{a}| \equiv 1, \quad (2.2)$$

which is exactly the Lagrangian formulation of the inviscid dynamics of an incompressible fluid. Note that Eq. (2.2) is second order in time, which means that we need two boundary conditions provided by the initial and final maps in Arnold’s principle (AVP).

## 2.2. Boundary-value formulation and turnover time

The boundary-value formulation of Arnold’s principle (AVP) is not usual in fluid mechanics. One rather considers the initial-value problem, which involves the initial fluid velocity  $\partial_t\mathbf{X}(\mathbf{a}, 0) = \mathbf{v}_0(\mathbf{a})$  in addition to the initial map. However, as we will now see, the connection between these two formulations is not univocal.

It is easily understood that for an infinitesimally short time lag  $t_f$ , there is a one-to-one correspondence between the initial velocity field and a final map that is sufficiently close to identity:  $\mathbf{X}_f \approx \mathbf{I} + t_f \mathbf{v}_0$ . This mapping actually extends to longer time lags and a given solution to the initial-value problem can then be retrieved by solving (AVP) with the appropriate boundary conditions. This is however true only up to a finite value  $t_\star$  of the time lag. The breakdown of the one-to-one correspondence for  $t_f > t_\star$  is clear when the flow is vortical. The critical time  $t_\star$  can be heuristically understood as a turnover time. Let us for instance consider a 2D solid-rotating flow in a disk of radius  $R$ . In Eulerian coordinates the velocity field reads

$$\mathbf{v}_\Omega(\mathbf{x}, t) = \Omega \times \mathbf{x} \quad \text{with } \Omega := \Omega \hat{\mathbf{z}} \text{ a prescribed (constant) vorticity.} \quad (2.3)$$

This is a steady solution to the Euler equations. The corresponding Lagrangian flow is obviously obtained as:

$$\mathbf{X}_\Omega(\mathbf{a}, t) = \mathbf{a} \cos \Omega t + \hat{\mathbf{z}} \times \mathbf{a} \sin \Omega t. \quad (2.4)$$

We can now seek to apply the boundary-value formulation (AVP) to reconstruct the rotating dynamics. The final map is naturally prescribed as  $\mathbf{X}(\cdot, t_f) = \mathbf{X}_\Omega(\cdot, t_f)$ . Observe that this end-point condition determines the rotation modulo  $2\pi$  only: Writing  $\theta_f \in ]-\pi, \pi]$  the principal value of the final angle  $\Omega t_f$ , it is readily seen that Arnold’s minimal flow is to be searched among the solid rotations with pulsation satisfying  $\Omega' t_f = \theta_f \bmod 2\pi$ , and corresponding action  $\mathcal{A}_{0,t_f} = (\pi/6)R^4 \Omega'^2 t_f$ . The minimising flow is such that  $\Omega' = \Omega_\star = \theta_f/t_f$ . This implies that Arnold’s minimiser univocally reproduces the desired Euler solution only if  $t_f < t_\star = \pi/\Omega$ . For  $t_f > t_\star$ , the minimizer is a solid-rotation with a smaller vorticity  $|\Omega_\star| < \Omega$  (see Fig. 1). The true solution still makes the action stationary but is not peculiar among the other critical points. Inducing from the solid-rotation example, it becomes intuitively clear that the presence of local rotation restricts the use of the boundary value formulation in terms of Lagrangian maps. In that sense, the critical time  $t_\star$  can be tied to a notion of turnover time. It will soon be apparent that this turnover time also plays a crucial role in Brenier’s formulation.

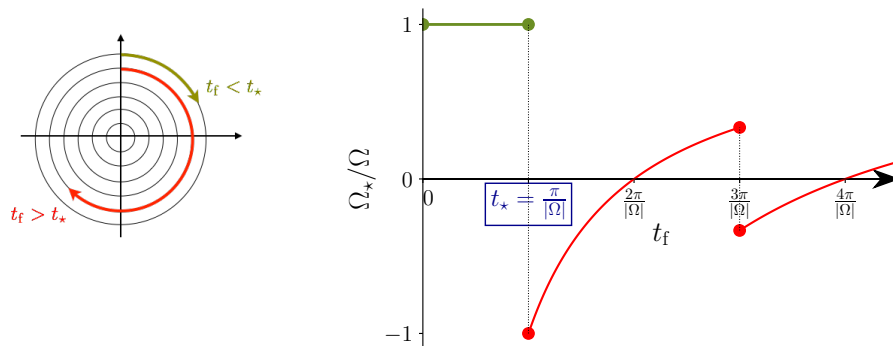


FIGURE 1. Attempts to reconstruct a solid-rotating flow with pulse  $\Omega$  from the variational principle (AVP) only yield the correct solution when  $t_f < t_*$  (in green) and the final map has rotated less than half a turn (left illustration). For  $t_f > t_*$  (in red), the reconstructed vorticity  $\Omega_*$  is lower and may even be of opposite sign. This can be seen on the right-hand panel, which shows the action-minimising vorticity  $\Omega_*$  as a function of the final time  $t_f$ .

### 2.3. Brenier’s least-action principle

As previously evoked, another restriction of Arnold’s description comes from its deterministic nature, even when  $t_f$  is small enough. In particular, the description of a fluid in terms of a flow map cannot appropriately reproduce the “rough” solutions to the Euler equations that could be of relevance for inertial turbulence.

In Brenier’s generalisation of (AVP), the fluid is no longer defined in terms of a Lagrangian flow map  $\mathbf{X}(\mathbf{a}, t)$ , but rather in terms of a *generalised flow*: namely, a *probability measure*  $\mu[\mathfrak{D}\gamma]$  defined over Lagrangian trajectories  $t \mapsto \gamma(t)$ . We only consider differentiable trajectories, so that one can define the time-integrated energy as

$$\mathcal{S}[\gamma] = \frac{1}{2} \int_0^{t_f} dt \|\partial_t \gamma(t)\|^2.$$

The Lagrangian random variable  $\mathcal{S}[\gamma]$  is now the fundamental “energy functional” quantity that generalises the action. Still, generalised flows also require generalised constraints. Essentially, we prescribe to a fixed distribution the two-time probability  $\mu|_{0,t_f}$  of  $t = 0$  and  $t = t_f$ , which is obtained as a marginal of  $\mu$ . As for the incompressibility constraint, it translates into imposing that the one-time distributions  $\mu|_t$ , given again by  $\mu$ , stay uniform as a function of time. Brenier’s least action principle can now be formally stated:

$$\mathcal{B}_{0,t_f}[\mu] := \int \mu[\mathfrak{D}\gamma] \mathcal{S}[\gamma] \longrightarrow \inf \quad \text{subject to} \quad (\text{BVP})$$

$$\mu|_{0,t_f} = \mu_{0,f} \quad \text{and} \quad \mu|_t \text{ uniform.}$$

The probabilistic constraints are on marginals of the distribution  $\mu$ , whence the relationship with multi-marginal optimal transport. Because there is a probabilistic coupling  $\mu_{0,f}$  between the initial and final positions, the formulation (BVP) is again a boundary-value problem.

The generalised least-action principle (BVP) was conceptualised by Brenier (1989) — see also Brenier (2008) —, with some established mathematical properties, including:

- (i) Generalised solutions to (BVP) exist for very general end-point couplings  $\mu_{0,f}$ .
- (ii) The generalised variational principle encompasses classical (regular) solutions, provided that the final time  $t_f$  is small enough. This requires choosing a deterministic end-point coupling, which is prescribed by the map associated to a solution to the Euler equations, *i.e.*  $\mu_{0,f}(\mathbf{d}\mathbf{a}, \mathbf{d}\mathbf{x}) = |\mathcal{D}|^{-1} \delta(\mathbf{X}_f(\mathbf{a}) - \mathbf{x}) \mathbf{d}\mathbf{a} \mathbf{d}\mathbf{x}$ . The solution to (BVP) is then highly degenerate, concentrated on the deterministic Lagrangian flow. This requires  $t_f < t_\star$  with

$$t_\star = \frac{\pi}{\sup_{\mathbf{x},t} \|\text{Hessian}(p)\|^{1/2}}, \quad (2.5)$$

with  $p$  denoting the pressure field appearing in the underlying Euler equations.

- (iii) For  $t_f > t_\star$ , generalised flows can become non-deterministic: The flow is no more described by the Lagrangian map, but rather by transition probabilities. A generalised “fluid particle” tagged by its initial position then splits mass and have a multiplicity of subsequent positions at time  $t$  prescribed by the two-time marginals  $\mu|_{0,t}$ .

Point (ii) above shows that (BVP) is indeed a generalisation of (AVP). Yet, the short-time restriction of Arnold’s boundary-value formulation remains: Seemingly, considering  $t_f > t_\star$  might not be of physical relevance. Note in passing that for a solid rotation the pressure field is  $p(x, y) = (\pi/2)(x^2 + y^2)$ , yielding in that case  $t_\star = \pi/|\Omega|$  as obtained in §2.2. In fact, the “generalised” aspect of (BVP) relates to the type of Euler solutions that it can construct. Those can in principle include weak solutions to the Euler equations, be them distributional or even measure-valued (Brenier 1999). In those cases, the generalised flow is always non-deterministic, even at short  $t_f$ .

In addition to those conceptual features, Brenier’s formulation has also a practical outcome : While (AVP) is a highly non-linear problem which is cumbersome to use in practice, (BVP) is a linear optimisation problem, that can in principle be tackled numerically. The relevance of generalised flows when used in combination with turbulent inputs can therefore be tested, and this remarkable feature provides the guideline for the remainder of the paper.

### 3. Statistical physics of generalised flows

The generalised variational principle (BVP) connects inviscid fluid mechanics with multimarginal optimal transport. Its numerical integration can thus benefit from the efficient algorithms that have been developed to solve such optimisation problems. In recent years, (BVP) has even been used as a testground in the development of such methods—see for instance Brenier (2008); Benamou *et al.* (2015, 2017); Nenna (2016); Gallouët & Mérigot (2018). Here we follow a different strategy. We rather rely on a Monte-Carlo algorithm, as the latter proves sufficient for our present scope. It stems from an intuitive statistical-mechanics interpretation of (BVP).

#### 3.1. Coarse-graining and permutation flows

It is illuminating to reformulate (BVP) in a discrete setting, both in space and in time. Specifically, we discretise time into  $N_t$  steps  $t_0 = 0, t_1, \dots, t_{N_t} = t_f$ , and partition the  $d$ -dimensional physical domain  $\mathcal{D}$  into  $N_x^d$  “boxes” of equal volume, and labeled by the  $d$ -dimensional indices  $\mathbf{i} = (i_1, \dots, i_d) \in [1, N_x]^d$ . In this “coarse-grained” description, Lagrangian trajectories become sequences of indices  $\{\mathbf{i}_n\}_{n=0..N_t}$ , and generalised flows become finite-dimensional tensors, represented by the non-negative  $(N_x^d)^{N_t}$  entries  $\mu\{\mathbf{i}_n\} := \mu(\mathbf{i}_0, \mathbf{i}_1, \dots, \mathbf{i}_{N_t})$  normalised to 1. One can now think of an *incompressible* generalised flow in two equivalent ways :

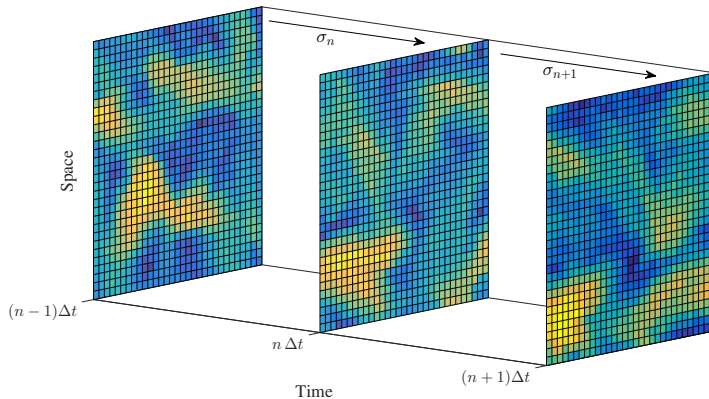


FIGURE 2. Illustration of a two-dimensional permutation flow.

(i) In the “Linear-programming viewpoint”, it is a measure with uniform single-time marginals (Nenna 2016), that is

$$\mu_k(\mathbf{i}_k) := \sum_{\mathbf{i}_0 \dots \mathbf{i}_{k-1}, \mathbf{i}_{k+1} \dots \mathbf{i}_{N_t}} \mu\{\mathbf{i}_n\} = 1/N_x^d, \quad \text{for all } k = 0..N_t. \quad (3.1)$$

(ii) In the “Statistical mechanics viewpoint”, it is a measure prescribed by a certain ensemble average over “permutation flows”  $\sigma$  (Brenier 2008), that is

$$\mu\{\mathbf{i}_n\} \equiv \frac{1}{N_x^d} \left\langle \prod_{k=1}^{N_t} \delta_{\mathbf{i}_k \sigma_k(\mathbf{i}_0)} \right\rangle_{\sigma} \quad (3.2)$$

In the previous formula, each  $\sigma_n$  is a permutation over the  $N_x^d$  boxes between step 0 and step  $n$ . Taking  $\sigma_0 = \mathbf{I}$ , the sequence  $\{\sigma_n(\mathbf{i})\}_{n=0..N_t}$  then represents the coarse-graining of a Lagrangian trajectory starting from box  $\mathbf{i}$ , and the sequence  $\sigma = \{\sigma_n\}_{n=0..N_t}$  is termed the “permutation flow” (see illustration in Fig. 2). With this second interpretation at hand, we can now reformulate (BVP) in terms of an optimal statistical ensemble of permutation flows.

### 3.2. Generalised solutions as statistical ensembles of permutation flows.

Each realisation of a permutation flow yields the discrete action :

$$\mathcal{A}_{0,N_t}[\sigma] = \sum_{n=1}^{N_t} \mathcal{E}_n \quad \text{with} \quad \mathcal{E}_n = \sum_{\mathbf{i}} \|\sigma_n(\mathbf{i}) - \sigma_{n-1}(\mathbf{i})\|^2, \quad (3.3)$$

where  $\|\mathbf{i} - \mathbf{j}\|$  denotes here the discrete distance in  $\mathbb{Z}^d$  between the centres of boxes  $\mathbf{i}$  and  $\mathbf{j}$ . We now formulate the discrete counterpart to (BVP) as an optimization over discrete measures  $p[\sigma]$  defining statistical ensembles of permutation flows:

$$\mathcal{B}_{0,N_t}[p] := \sum_{\sigma} \mathcal{A}_{0,N_t}[\sigma] p[\sigma] \longrightarrow \inf \quad \text{subject to} \quad \sum_{\sigma} \sigma_{N_t} p[\sigma] = \mu_{0 \rightarrow t_f}, \quad (\text{BDVP})$$

where  $\mu_{0 \rightarrow t_f}$  is the transition probability from initial to final time. Using the standard matrix representation of permutations,  $\mu_{0 \rightarrow t_f}$  is an  $N_x^d \times N_x^d$  doubly stochastic matrix. The discrete formulation (BDVP) reveals that Brenier’s formulation resembles an averaged Arnold’s principle, whereby averages are taken with respect to measure-preserving applications, a set which includes but is not restricted to smooth volume-preserving maps.



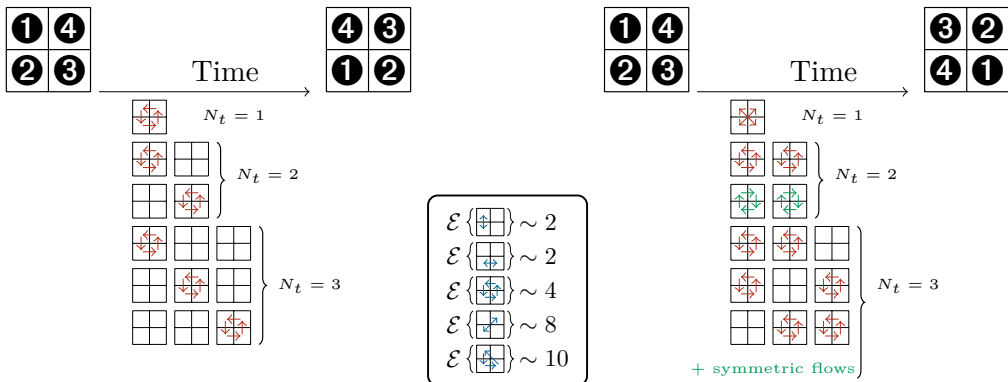


FIGURE 3. The solid rotation example, this time interpreted as a general permutation flow on a coarse  $(2 \times 2)$ -box: nothing but a sliding puzzle. The middle inset provides the energy cost of the representative elementary permutations. The left-hand panel shows the support of the optimal permutation flows obtained for various time discretisations, when the final permutation represents a quarter of a full turn. The right-hand panel shows the same with the final permutation now representing half a turn. In both cases, the supports obtained for large “ $N_t$ ” include non-physical permutation flows with “heart-beat” dynamics.

The optimal statistical measure that solves (BDVP) is discrete, but its dimensionality is huge†! Monte-Carlo algorithms are thus particularly suited to obtain numerical estimates of averages with respect to the optimal flow. Specifically, the formulation (BDVP) can be formally understood as the zero-temperature/infinite- $\beta$  limit of the Gibbs canonical measure

$$p_\beta[\sigma] = \frac{1}{Z(\beta)} e^{-\beta \mathcal{A}_{0, N_t}[\sigma]} \quad \text{with associated averages } \langle \cdot \rangle_\beta. \quad (3.4)$$

For finite temperatures, Monte-Carlo averages are then easily sampled using a local Metropolis algorithm (see, e.g., Binder 1986) on a  $(d + 1)$ -dimensional lattice, with the extra dimension representing the time axis. We note that the finite-temperature regularisation is probably a statistical-mechanics counterpart to the concept of entropic regularisation used by Nenna (2016) to implement efficient iterative projection algorithms rooted in the “Linear programming viewpoint”.

### 3.3. Large-time limit of optimal permutation flows.

From the perspective of discrete permutation flows, it is again apparent that (BDVP) should essentially become non-physical when the final time is too large. To hint at this behaviour, one can revisit the solid rotation example of §2.2, in terms of a very coarse generalised flow involving a  $(2 \times 2)$ -spatial discretisation and  $N_t$  time steps of length  $\Delta t$ . Figure 3 represents the support of the permutation flows for various  $N_t$ , when the final state is either a quarter or half of a full turn. In both cases, it is apparent that the generalised flow only describes a pure deterministic rotation when  $N_t$  is small. For larger  $N_t$ , it includes non-energy-preserving “heart-beat” dynamics: The rotation steps can be placed anywhere in the sequence of permutations connecting the initial and final ends, without changing the overall energy costs. This toy argument suggests that there should be no physical meaning for the generalised variational formulation at large times: With that hint in mind, we can now study the physical properties of more intricate generalised flows, for which the vorticity field is no longer a mere constant of space and time.

† explicitly :  $(N_x^d)!^{N_t}$ .

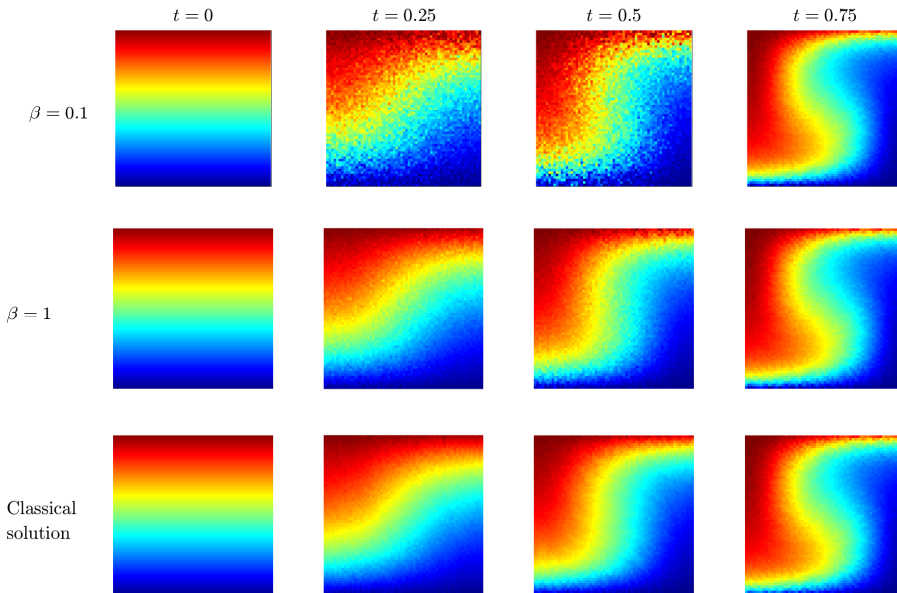


FIGURE 4. Reconstruction of the Beltrami dynamics as a function of time and  $\beta$  for  $t_f = 0.75 < t_*$ . The colour code stands for the initial  $y$  position of fluid particles.

#### 4. Generalised flows and Beltrami dynamics

Beltrami flows are a class of strong Euler solutions of next-order complexity compared to solid rotations : While stationary, their vorticity is not constant in space. It is therefore instructive to study the statistical features of the generalised flows induced when using Beltrami Lagrangian map as boundary conditions. Using our Monte-Carlo algorithm, we find that the generalised flows indeed reproduce the intermediate Lagrangian dynamics of Beltrami flows for small times. For large final times, the Lagrangian flow breaks down. Even if this could have a promising “turbulent flavour” and provide a possible framework to model intrinsic stochasticity, a deeper analysis of their statistical features reveals that such generalised flow are actually unphysical.

##### 4.1. Generalised flows from Beltrami maps

We consider the one-cell Beltrami flow defined by the Eulerian velocity field on the domain  $\mathcal{D} = [0, 1]^2$ :

$$\mathbf{v}(\mathbf{x}, t) = (\cos \pi y \sin \pi x, -\cos \pi x \sin \pi y)^\top, \quad (4.1)$$

from which we obtain explicitly  $t_* = 1$  using Brenier’s formula (2.5). Tracer particles are used to generate Beltrami permutation maps on a  $64^2$  spatial grid at different prescribed final times. The generalised flows are then constructed with fixed time-step  $\Delta t = t_*/8$ . For instance, when  $t_f = t_*$ , the discretisation has parameters  $N_x = 64$  and  $N_t = 8$  in the notations of §3. To ensure that a statistical steady state is attained, averages are computed after routinely discarding the first  $10^6$  Monte-Carlo times<sup>†</sup>, and then using the data generated over the next  $2.5 \times 10^5$  ones. Our numerics clearly show that  $t_* = 1$  marks a transition between a deterministic and a stochastic regime for the generalised flow.

<sup>†</sup> One Monte-Carlo time is standardly defined as  $N_x^2 \times N_t$  iterations of the algorithm.

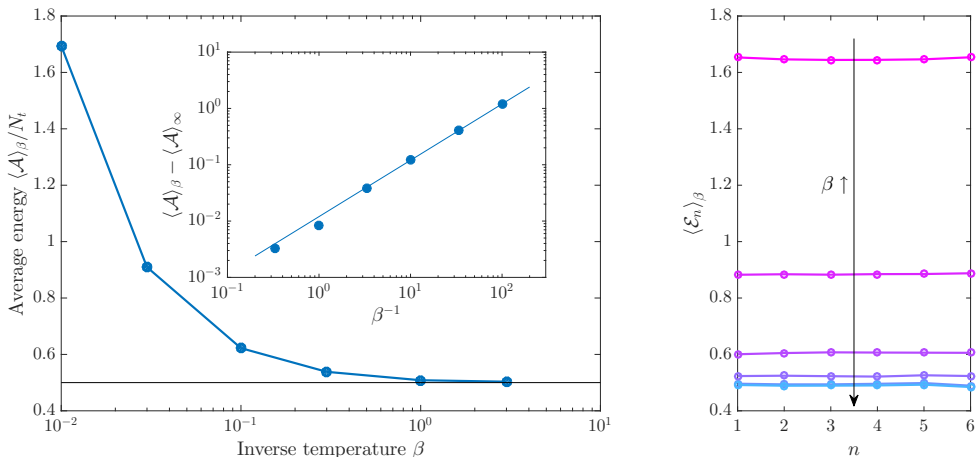


FIGURE 5. Convergence of the action for the case  $t_f < t_*$ . The left-hand panel shows convergence at zero temperature of the time-averaged kinetic energy—given by the action in (BDVP)—towards the optimal Beltrami action. The right-hand panel shows the time dependence of the generalised flow energy for inverse temperatures  $\beta = 0.01, 0.03, 0.1, 0.3, 1$  and  $3$  (from top to bottom).

#### 4.2. $t_f < t_*$ : Convergence toward Beltrami dynamics.

When  $t_f < t_*$ , it is found that the Gibbs measures  $\langle \cdot \rangle_\beta$  concentrate around the deterministic dynamics in the limit of zero temperature,  $\beta \rightarrow \infty$ . This can be seen in Fig. 4: For small-enough temperatures, the average Lagrangian maps become essentially undistinguishable from those associated to the deterministic Beltrami flows, up to some small remaining thermal noise. This convergence towards the optimal ensemble is shown more clearly in Fig. 5: As  $\beta$  increases, the average action converges towards the Beltrami action, which, as we know, solves (BDVP) when  $t_f < t_*$ . As shown in inset, the convergence is algebraic  $\propto \beta^{-1}$ . Moreover, it is apparent from the right-hand panel of Fig. 5 that energy is conserved in time. This is a signature of the high regularity of such a classical solution to the Euler equations. This observed regularity is a consequence of the variational principle and was definitely not prescribed. This shows the effectiveness of Brenier’s variational principle to accommodate strong, classical, deterministic solutions, in spite of its probabilistic nature. Finally, let us note that the “finite temperature effects” are apparent on the spectra of the displacement and translate into small-scale thermalisation, namely equipartition of energy (see the left-hand panel of Fig. 6). The range of thermalised scales naturally decreases with increasing  $\beta$ . Those features show the roundabout behaviour of our numerical procedure. They illustrate the established fact that for small enough  $t_f < t_*$  the generalised formulation (BVP) do indeed reproduce the Arnold’s minimisers of (AVP) when those exist, as proven in Brenier (1989).

#### 4.3. $t_f > t_*$ : Non-physical behaviour of the generalised flow.

When  $t_f > t_*$ , the behaviour of the generalised flow becomes non-deterministic, and the time-conservation of energy breaks down—see Fig. 7. This implies in particular that generalised flows cannot solve the Euler equations in a strong sense anymore. Yet, it is also apparent that the flow is not *dissipative*: The variations in the energy profile shown in the lower panel are symmetric and localised at the boundaries. Those behaviours are non-physical and likely consequences of both the time-symmetry and the boundary-value formulation of the principle (BVP) itself. In the example chosen for Fig. 7, the

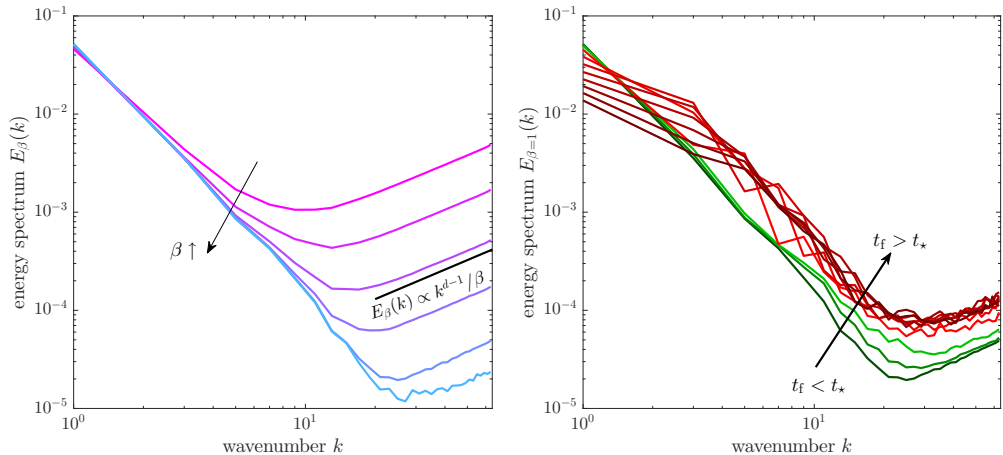


FIGURE 6. Kinetic energy spectra for, on the left-hand panel,  $t_f < t_*$  and various  $\beta$  (same values as Fig. 5 left) and, on the right-hand panel, for  $\beta = 1$  fixed and various  $t_f$  ranging from 0.75 up to 2 every 0.125. The curves corresponding to  $t_f < t_*$  are shown in green, the others in red.

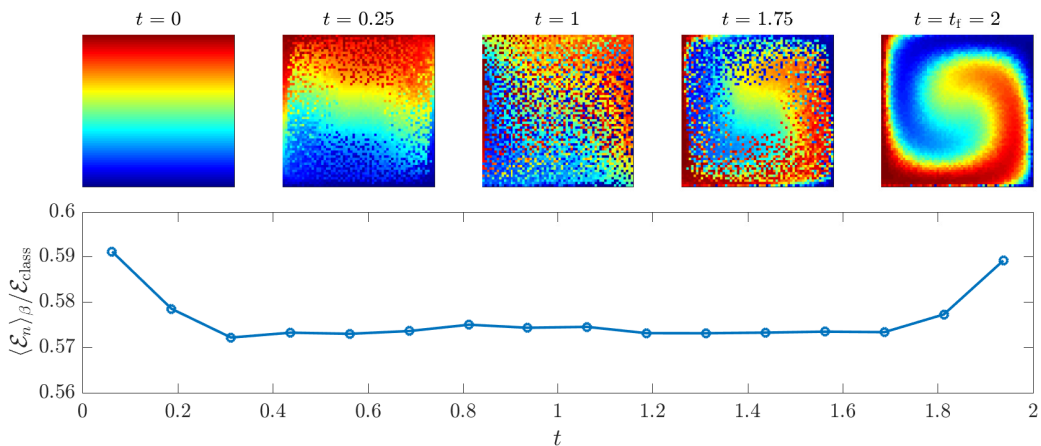


FIGURE 7. Upper panel: typical permutation flow for the generalised solution with  $t_f = 2t_*$ . We again show here, as a coloured background, the initial  $y$  label as a function of time. Lower panel: time-evolution of the kinetic energy. It is no longer conserved, and exhibits strong variations at the time boundaries.

breakdown of the Lagrangian flow is particularly spectacular for  $t = t_f/2 = 1$ . The nearly-uniform colour pattern shows that initially distant pockets of fluid become arbitrarily close to each other at intermediate times before separating again. This is the signature of trajectory crossings. This picture may misleadingly suggest that generalised solutions essentially produce a thermalised dynamics, with fluid motion occurring at random. This is however not the case, as revealed by looking at the Eulerian spectra of the generalised displacement that are displayed in the right-hand panel of Fig. 6. While the small scales are indeed thermalised, the thermalisation is rather likely a spurious finite-temperature effect due to our numerical procedure, as its spread in  $k$ -space is not much wider than in the  $t_f < t_*$  case. The generalised flows obtained for  $t_f > t_*$  however display specific large-scale dynamics, which carry far less energy than the deterministic counterparts, whence their selections as optimal flows. We also note that, apart in the spurious thermalised

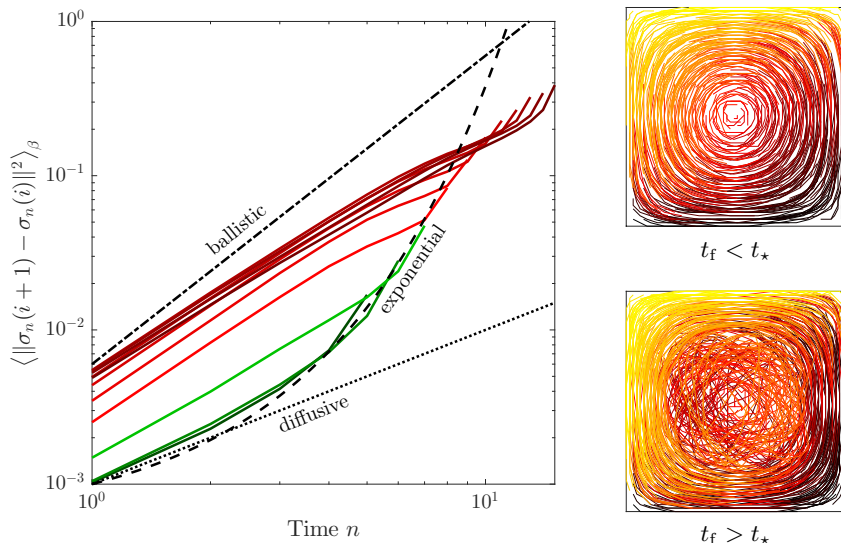


FIGURE 8. Left: Average Lagrangian displacement for both  $t_f < t_*$  (green)  $t_f > t_*$  (red). Right: realisations of the Lagrangian trajectories, again for time lags  $t_f$  below (top) and above (down) the critical time  $t_*$ .

range, the specific scalings displayed by the Beltrami generalised flows have no known counterparts in the phenomenology of two-dimensional turbulence.

Perhaps, this is even better seen from the Lagrangian measurements shown in Fig. 8. As can be seen on the left-hand panel, the motions of fluid particles transit from a diffusive towards a faster ballistic regime when  $t_f$  is increased. The present breakdown of the Lagrangian flow is therefore not related to the phenomenon of explosive turbulent separation, nor to Richardson’s diffusion. The origin of a ballistic behaviour can actually be identified by looking at specific realisations of the generalised Beltrami trajectories. One indeed observes on the right-hand panels of Fig. 8 that for  $t_f > t_*$  that trajectories located at the center of the domain “tunnel” through the large-scale vortex to reach almost ballistically their final prescribed location. The statistics is then dominated by such displacements, which prove more efficient at transporting energy than classical rotating motions. Deviations to a purely ballistic regime come from the Lagrangian trajectories in a thin layer near the domain boundary, which remain “classical”: This is likely a consequence of the non-uniform distribution in Beltrami flows of vorticity, which is weaker at the boundary than at the center of the domain.

#### 4.4. Comments

The statistical analysis on generalised Beltrami flows confirms the intuition built from the  $(2 \times 2)$  solid-rotation model considered in §3.3: The transition from deterministic to non-deterministic generalised flows is not at any rate a transition to turbulence, however appealing this would have sounded. The generalised flows above  $t_*$  display a number of non-physical features, ranging from non-monotonous sharp variations of the energy at initial and final times, to “vortex-tunneling” ballistic motions of fluid trajectories. These highly undesirable specificities could possibly be avoided by further constraining the Lagrangian variational principle. For example, one can break the time-symmetric formulation by enforcing that energy be decreasing. On the one hand, this path could likely be a dead-end as it is clear, already for Arnold’s regular geodesic, that the “ $t_*$  barrier” is a defect of the boundary-value formulation, but not of the least-action

principle. On the other hand, further constraining the Lagrangian trajectories may allow to formulate Brenier’s principle as a non-trivial free-end optimisation problem (namely an initial value problem in the language of partial differential equations), hereby wiping off artefacts due to the boundary-value formulation. At this point, our results therefore suggest that variational reconstructions of intermediate (turbulent) dynamics cannot rely solely on (BVP). It also requires an amount of data that ensures sufficiently close time-boundary conditions. Only at this price can one obtain a non-spurious “ $t < t_*$ ” behaviour. With that in mind, we next apply least-action principles to turbulent data.

## 5. Generalised flows and decaying 2D turbulence

The next step of our approach is to consider even more realistic cases where vorticity varies not only in space, but also in time. This is natural when one has in mind turbulent dynamics. Yet, the least-action principle that we have discussed is restricted to velocity fields solving the Euler equations. The classical solutions that were considered so far are of limited relevance to turbulent flows. In particular, they are too regular to occur as non-trivial limits of solutions to the Navier–Stokes equations when the viscosity  $\nu \rightarrow 0$ . In that context, it is believed that weak (irregular) solutions to the Euler equations are more suitable candidates. Generalised least-action principle would be particularly useful if they could be used to tackle such non-smooth velocity fields. We naturally have in mind the possibility of addressing three-dimensional flows, but we here restrict ourselves to the problem of the two-dimensional direct enstrophy cascade.

It has been known since Batchelor (1969) that two-dimensional turbulence does not dissipate kinetic energy when the viscosity tends to zero. In the absence of forcing, there is however another inviscid invariant, namely the enstrophy  $Z$  defined as the space integral of the square of the vorticity  $\omega = \partial_x v_y - \partial_y v_x$ . Batchelor’s scaling predicts that the enstrophy displays a dissipative anomaly but this requires approaching the inviscid limit with an infinite enstrophy (see Eyink 2001). While these questions are still not fully settled (see Lopes Filho *et al.* 2006; Dmitruk & Montgomery 2005; Vigdorovich 2018), one can reasonably expect that two-dimensional, decaying, turbulent velocity fields are irregular solutions to the Euler equations. This, together with the absence of kinetic energy dissipation, motivates applying to that case the generalised least-action principle. Let us note that the presence of a finite enstrophy dissipation in the limit of vanishing viscosity makes the dynamics time irreversible. It is a priori unclear if and how this feature will be accommodated by Brenier’s principle.

We perform direct numerical simulations of the decaying two-dimensional Navier–Stokes equations. The initial velocity field, with energy  $E(0)$  and enstrophy  $Z(0)$ , is chosen from another set of simulations where both a large-scale random forcing and linear friction are present. We use a pseudo-spectral solver with  $256^2$  collocation points and kinematic viscosity  $\nu = 10^{-3}$ . We embed 250,000 tracers and compute permutation flows  $\{\sigma_n\}$  on a  $N_x^2 = 64^2$  coarse-grained grid every  $t_f = Z^{-1/2}(0)$ . This is the smaller timescale of the flow. The two-dimensional direct cascade is indeed characterised by a single turnover time prescribed by the enstrophy.

The obtained permutation flow provides boundary conditions for the generalised least-action principle. We use the Metropolis algorithm of §3.2 to reconstruct the velocity field at five intermediate times between  $n t_f$  and  $(n + 1) t_f$ . Figure 9 illustrates this procedure for  $n = 0$ . The vorticity field at time  $t_f$  obtained from the direct simulations is shown on the left-hand panel. The central panel shows a realisation of the reconstructed vorticity  $\bar{\omega}$  for an inverse temperature  $\beta = 1$ , and without any averaging. It is obtained by finite differences of the Lagrangian displacement, and one can hardly distinguish any structure.

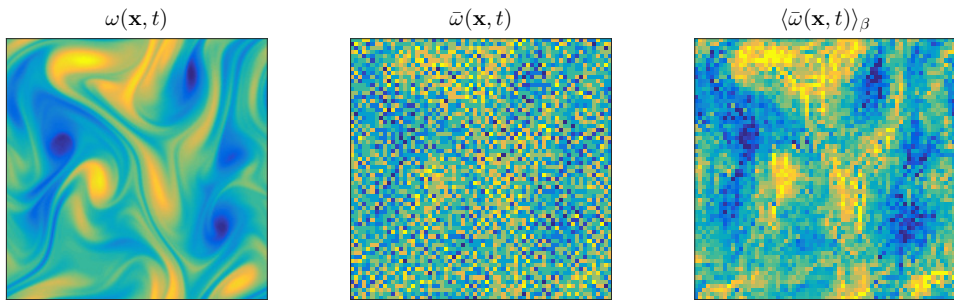


FIGURE 9. Snapshot of the vorticity field at time  $t = t_f/2$ . Positive values are shown in blue and negative ones in yellow. The left-hand panel is the original vorticity field obtained from the direct numerical simulation with  $256^2$  collocation points. The centre panel is a fluctuating realisation of the reconstructed vorticity on a  $64^2$  coarse graining with a finite temperature  $\beta^{-1} = 1$ . The right-hand panel is the generalised flow approximation obtained by averaging over the Gibbs ensemble.

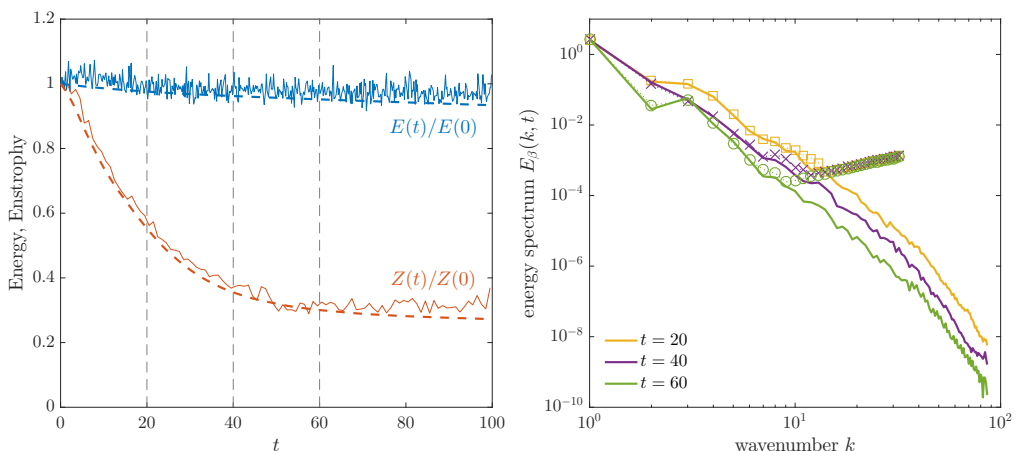


FIGURE 10. Left: Energy and enstrophy as a function of time both for the actual field (dashed lines) and the reconstructed one (thin solid lines). Here,  $Z(t)$  is averaged over the reconstructed time intervals  $[n t_f, (n+1) t_f]$ , while  $E(t)$  is not, whence the stronger fluctuations for the second. Time is here in units of  $Z^{-1/2}(0)$ . Right: kinetic energy spectra of both the original velocity field (solid lines) and of the reconstructed one (dashed lines with symbols) at different times, as labeled.

It is only after averaging over  $10^6$  Monte-Carlo times that one smears out the noise. The spatial organisation of the original flow is indeed recovered on the right-hand panel of Fig. 9, which displays the Gibbs-averaged vorticity  $\langle \bar{\omega} \rangle_\beta$ . The blurry aspect is due to the finite value of temperature. The generalised vorticity will be formally obtained for  $N_x, N_t \rightarrow \infty$ , together with  $\beta \rightarrow \infty$ .

This procedure is repeated up to  $n = 100$ . Figure 10 (left) shows the time evolution of the kinetic energy  $E(t)$  and of the enstrophy  $Z(t)$ . Data from the direct simulation (shown as dashed lines) show that the enstrophy decreases abruptly while energy is almost conserved. This confirms that our settings correspond to the small-viscosity limit of two-dimensional decaying turbulence. The slow decrease of  $E(t)$  is due to the tiny amount of viscous dissipation used in the numerics. The solid lines are the energy and enstrophy obtained from the reconstructed flow. We observe that the global decay is

properly reproduced with superimposed fluctuations due to a finite temperature. Other deviations might be due to statistical errors in the ensemble average or to the discreteness of the reconstructed field. The scaling properties of the velocity fields can be examined from the energy power spectra shown in the right-hand panel of Fig. 10. Data show an excellent agreement at large scales. As observed earlier in Beltrami flows, reconstructed fields display a  $\propto k$  range at small scales. The crossover wavenumber apparently decreases with time, so that one can expect a full thermalisation at large times. The quality of the reconstruction will thus deteriorate, as can be already inferred from the left-hand panel at times  $t \gtrsim 70$ .

These attempts at using Brenier's principle to reconstruct weak solutions to the Euler equations are rather promising. In particular, this approach seems suited to capture irreversible dynamics, and is hence compatible with the concept of dissipative inviscid solutions. Nevertheless, one should be aware that the reconstructed data is here very regular compared to a genuine turbulent three-dimensional flow. While this still constitutes a first step, the observables that we considered are dominated by the larger scales, with a velocity field that apparently remains very close to a classical solution of the inviscid dynamics.

## 6. Concluding remarks

In spite (or because) of its high degree of universality, Brenier's generalised least-action principle has so far hardly found any practical application in the realm of fluid mechanics, let alone for turbulence modeling. In fact, our analysis highlights one of its main limitation, namely its formulation in terms of a two-end boundary-value problem in time. While Brenier's generalised framework guarantees the existence of geodesics for all times, the non-deterministic properties of the minimising flows that appear when  $t_f > t_*$  is essentially an artefact of the boundary-value formulation itself. In that regime, generalised flows are found to be unphysical and therefore useless for turbulence.

Such is however not the case in the regime  $t_f < t_*$ . Our work illustrates that Brenier's generalised least-action principle (BVP) is then not only useful but also highly versatile. Specifically, it can be used as an efficient reconstruction device, in order to a posteriori approximate various classes of inviscid dynamics and reconstruct Lagrangian trajectories. This essentially comes from the fact that compared to Arnold's formulation (AVP), the optimisation problem (BVP) is largely unconstrained. In particular, the probabilistic framework does not require any assumption about the smoothness of the minimising flow. This desirable feature makes it particularly suitable as a coarse-graining tool, as Brenier's formulation naturally carries through on discrete settings, both in space and in time — at sharp contrast with Arnold's formulation. Besides, the optimising space is sufficiently large, so that minimising algorithms can converge efficiently, without getting trapped within local minima. As such, it may now come as no surprise that simple Monte-Carlo strategies, such as the one presented in §3, yield faithful approximates to (BVP).

The inviscid dynamics that lie within the scope of Brenier's action principle include the strong solutions captured by Arnold's principle, in which case the minimising generalised flow becomes degenerate as it concentrates on the deterministic solution. More interestingly, the numerical analysis presented in §5 suggests that Brenier's principle may also reproduce irreversible dynamics that are a priori prescribed by weak solutions to the Euler equation. In our view, this numerical evidence is very promising. In particular, it paves the way towards new tools where generalised flows are used to



coarse-grain fully turbulent dynamics.

Although it is yet unclear to us what  $t_*$  is when the dynamics is multi-scale, a long-term plan could be to address three-dimensional solutions to the incompressible Navier–Stokes equations in the vanishing viscosity limit. Beside data analysis and models, generalised least-action principles could provide a natural statistical mechanics framework to relate the time-irreversibility of turbulence to the explosive nature of Lagrangian separations (Richardson’s dispersion). More speculatively, it could even possibly unveil some new Lagrangian symmetries. For example, among the fundamental consequences of the Lagrangian variational formulation *à la* Arnold is the existence of Lagrangian Noether currents, namely inviscid conservation laws that stem from continuous symmetries of the action. Of particular relevance for ideal fluids is the “relabelling symmetry” (Shepherd 1990; Padhye & Morrison 1996), namely the seemingly trivial observation that the dynamics should not depend on the specific continuous labels assigned to the fluid particles. This symmetry translates into the Kelvin’s and Ertel’s circulation theorems for barotropic and baroclinic flows respectively (Salmon 1988; Frisch & Villone 2014). It would be of particular interest to derive from Brenier’s generalised least-action principle some suitable probabilistic analogues of such smooth Lagrangian conservation laws, as those could then be tested explicitly using coarse-grained data from DNS or experiments.

This overall perspective naturally relies on the crucial assumption that turbulence is described by weak solutions to the Euler equations. If such was indeed the case, generalised flows would then provide a natural framework to think of turbulent solutions in terms of Lagrangian transition probabilities.

## REFERENCES

- ABARBANEL, H. D., HOLM, D. D., MARSDEN, J. E. & RATIU, T. S. 1986 Nonlinear stability analysis of stratified fluid equilibria. *Phil. Trans. R. Soc. Lond. A* **318** (1543), 349–409.
- ANTONIA, R. A. & BURATTINI, P. 2006 Approach to the 4/5 law in homogeneous isotropic turbulence. *J. Fluid Mech.* **550**, 175–184.
- ARNOLD, V. I. 1966 Sur la géométrie différentielle des groupes de lie de dimension infinie et ses applications à l’hydrodynamique des fluides parfaits. *Ann. Inst. Fourier* **16**, 319–361.
- ARNOLD, V. I. 2013 *Mathematical methods of classical mechanics, Graduate Texts in Mathematics*, vol. 60. New York: Springer.
- BATCHELOR, G. K. 1969 Computation of the energy spectrum in homogeneous two-dimensional turbulence. *Phys. Fluids* **12**, II–233.
- BENAMOU, J.-D., CARLIER, G., CUTURI, M., NENNA, L. & PEYRÉ, G. 2015 Iterative Bregman projections for regularized transportation problems. *SIAM J. Sci. Comput.* **37**, A1111–A1138.
- BENAMOU, J.-D., CARLIER, G. & NENNA, L. 2017 Generalized incompressible flows, multi-marginal transport and Sinkhorn algorithm. ArXiv preprint arXiv:1710.08234.
- BINDER, K. 1986 Introduction: Theory and technical aspects of Monte Carlo simulations. In *Monte Carlo Methods in Statistical Physics*, pp. 1–45. Berlin, Heidelberg: Springer.
- BOUCHET, F. & CORVELLEC, M. 2010 Invariant measures of the 2d euler and vlasov equations. *J. Stat. Mech. Theory Exp.* **2010**, P08021.
- BOUCHET, F. & VENAÏLLE, A. 2012 Statistical mechanics of two-dimensional and geophysical flows. *Phys. Rep.* **515**, 227–295.
- BRENIER, Y. 1989 The least action principle and the related concept of generalized flows for incompressible perfect fluids. *J. Am. Math. Soc.* **2**, 225–255.
- BRENIER, Y. 1999 Minimal geodesics on groups of volume-preserving maps and generalized solutions of the Euler equations. *Commun. Pure Appl. Math.* **52**, 411–452.
- BRENIER, Y. 2008 Generalized solutions and hydrostatic approximation of the Euler equations. *Physica D* **237**, 1982–1988.

- BRENIER, Y., DE LELLIS, C. & SZÉKELYHIDI, L. 2011 Weak-strong uniqueness for measure-valued solutions. *Commun. Math. Phys.* **305**, 351–361.
- BUCKMASTER, T. 2015 Onsagers conjecture almost everywhere in time. *Commun. Math. Phys.* **333**, 1175–1198.
- BUCKMASTER, T., LELLIS, C. & SZÉKELYHIDI, L. 2016 Dissipative Euler flows with Onsager-critical spatial regularity. *Commun. Pure Appl. Math.* **69**, 1613–1670.
- DIPERNA, R. J. & MAJDA, A. J. 1987 Oscillations and concentrations in weak solutions of the incompressible fluid equations. *Commun. Math. Phys.* **108**, 667–689.
- DMITRUK, P. & MONTGOMERY, D. C. 2005 Numerical study of the decay of enstrophy in a two-dimensional navier–stokes fluid in the limit of very small viscosities. *Phys. Fluids* **17**, 035114.
- DUCHON, J. & ROBERT, R. 2000 Inertial energy dissipation for weak solutions of incompressible Euler and Navier-Stokes equations. *Nonlinearity* **13**, 249–255.
- EBIN, D. G. & MARSDEN, J. 1970 Groups of diffeomorphisms and the motion of an incompressible fluid. *Ann. Math.* **92**, 102–163.
- EYINK, G. L. 2001 Dissipation in turbulent solutions of 2D Euler equations. *Nonlinearity* **14**, 787–802.
- EYINK, G. L. 2002 Local 4/5-law and energy dissipation anomaly in turbulence. *Nonlinearity* **16**, 137–145.
- EYINK, G. L. & SREENIVASAN, K. R. 2006 Onsager and the theory of hydrodynamic turbulence. *Rev. Mod. Phys.* **78**, 87–135.
- FALKOVICH, G., GAWEŹDKI, K. & VERGASSOLA, M. 2001 Particles and fields in fluid turbulence. *Rev. Mod. Phys.* **73**, 913–975.
- FRISCH, U. & VILLONE, B. 2014 Cauchy's almost forgotten Lagrangian formulation of the Euler equation for 3D incompressible flow. *Eur. Phys. J. H* **39**, 325–351.
- GALLOUËT, T. & MÉRIGOT, Q. 2018 A lagrangian scheme à la Brenier for the incompressible Euler equations. *Foundations of Computational Mathematics* **18**, 835–865.
- GAWEŹDKI, K. 2001 Turbulent advection and breakdown of the lagrangian flow. In *Intermittency in Turbulent Flows* (ed. J.C. Vassilicos), pp. 86–104. Cambridge: Cambridge University Press.
- HOLM, D. D. & KUPERSHMITD, B. A. 1983 Noncanonical Hamiltonian formulation of ideal magnetohydrodynamics. *Physica D* **7**, 330–333.
- HOLM, D. D., MARSDEN, J. E., RATIU, T. & WEINSTEIN, A. 1985 Nonlinear stability of fluid and plasma equilibria. *Phys. Rep.* **123**, 1–116.
- ISETT, P. 2018 A proof of Onsager's conjecture. *Ann. Math.* **188**, 871–963.
- JOSÉ, J. & SALETAN, E. 2000 *Classical dynamics: a contemporary approach*. Cambridge: Cambridge University Press.
- KHESIN, B. & ARNOLD, V. I. 2005 Topological fluid dynamics. *Notices Am. Math. Soc.* **52**, 9–19.
- KRAUS, M., TASSI, E. & GRASSO, D. 2016 Variational integrators for reduced magnetohydrodynamics. *J. Comput. Phys.* **321**, 435–458.
- LOPES FILHO, M. C., MAZZUCATO, A. L. & NUSSENZVEIG LOPES, H. J. 2006 Weak solutions, renormalized solutions and enstrophy defects in 2d turbulence. *Arch. Ration. Mech. Anal.* **179**, 353–387.
- MARSDEN, J. E. & WEST, M. 2001 Discrete mechanics and variational integrators. *Acta Numer.* **10**, 357–514.
- MÉRIGOT, Q. & MIREBEAU, J.-M. 2016 Minimal geodesics along volume-preserving maps, through semidiscrete optimal transport. *SIAM J. Numer. Anal.* **54**, 3465–3492.
- MILLER, J., WEICHMAN, P. B. & CROSS, M. C. 1992 Statistical mechanics, Eulers equation, and Jupiters red spot. *Phys. Rev. A* **45**, 2328–2359.
- MORRISON, P. J. 1998 Hamiltonian description of the ideal fluid. *Rev. Mod. Phys.* **70**, 467–521.
- MORRISON, P. J. 2005 Hamiltonian and action principle formulations of plasma physics. *Phys. Plasmas* **12**, 058102.
- NENNA, L. 2016 Numerical methods for multi-marginal optimal transportation. PhD thesis, PSL Research University.
- ONSAGER, L. 1949 Statistical hydrodynamics. *Nuovo Cimento* **6**, 279–287.

- PADHYE, N. & MORRISON, P. J. 1996 Fluid element relabeling symmetry. *Phys. Lett. A* **219**, 287–292.
- ROBERT, R. & SOMMERIA, J. 1991 Statistical equilibrium states for two-dimensional flows. *J. Fluid Mech.* **229**, 291–310.
- SALMON, R. 1983 Practical use of Hamilton’s principle. *J. Fluid Mech.* **132**, 431–444.
- SALMON, R. 1985 New equations for nearly geostrophic flow. *J. Fluid Mech.* **153**, 461–477.
- SALMON, R. 1988 Hamiltonian fluid mechanics. *Annual Rev. Fluid Mech.* **20**, 225–256.
- SAW, E.-W., DEBUE, P., KUZAY, D., DAVIAUD, F. & DUBRULLE, B. 2018 On the universality of anomalous scaling exponents of structure functions in turbulent flows. *J. Fluid Mech.* **837**, 657–669.
- SHEPHERD, T. G. 1990 Symmetries, conservation laws, and Hamiltonian structure in geophysical fluid dynamics. In *Adv. Geophys.*, , vol. 32, pp. 287–338. Elsevier.
- SHNIRELMAN, A. 2000 Weak solutions with decreasing energy of incompressible euler equations. *Commun. Math. Phys.* **210**, 541–603.
- SREENIVASAN, K. R. 1984 On the scaling of the turbulence energy dissipation rate. *Physics Fluids* **27**, 1048–1051.
- VIGDOROVICH, I. 2018 Enstrophy spectrum in freely decaying two-dimensional self-similar turbulent flow. *Phys. Rev. E* **98**, 033110.
- VILLANI, C. 2009 *Optimal transport: old and new*, *Grundlehren der mathematischen Wissenschaften*, vol. 338. Berlin Heidelberg: Springer-Verlag.
- ZEITLIN, V. 2004 Self-consistent finite-mode approximations for the hydrodynamics of an incompressible fluid on nonrotating and rotating spheres. *Phys. Rev. Lett.* **93**, 264501.